

Determination of $E2$ and $E4$ transition moments in $^{232}\text{Th}^\dagger$

C. Baktash and J. X. Saladin

University of Pittsburgh, Pittsburgh, Pennsylvania 15260

(Received 28 May 1974)

In a precision Coulomb excitation experiment, 16.5 and 17.0 MeV ^4He projectiles were employed to measure the electric quadrupole and hexadecapole transition matrix elements of the ground state rotational band of ^{232}Th . The results are $\langle 0^+ || \mathfrak{M}(E2) || 2^+ \rangle = 3.035 \pm 0.030 \text{ eb}$ and $\langle 0^+ || \mathfrak{M}(E4) || 4^+ \rangle = 1.36 \pm 0.14 \text{ eb}^2$. Model-dependent β_2 and β_4 deformation parameters are then extracted.

$$\left[\begin{array}{l} \text{NUCLEAR REACTIONS } ^{232}\text{Th}(\alpha, \alpha'), E = 16.5 \text{ and } 17 \text{ MeV measured } \sigma(E_{\alpha'}) / \\ \sigma(E_{\alpha}) \text{ for } \theta = 143, 170.5; \text{ deduced } \langle 0^+ || \mathfrak{M}(E2) || 2^+ \rangle, \langle 0^+ || \mathfrak{M}(E4) || 4^+ \rangle. \\ \text{Extracted model-dependent deformations } \beta_2 \text{ and } \beta_4. \end{array} \right]$$

I. INTRODUCTION

The presence of sizeable hexadecapole deformations in the actinide region ($228 \leq A \leq 250$) was first suggested by Fröman,¹ and later substantiated by several theoretical calculations.²⁻⁴ More recent investigations have provided theoretical estimates of the β_4 deformation for the actinide nuclei,⁵⁻⁷ as well as the "superheavy" nuclei.⁸ These calculations show that β_4 deformations can affect nuclear properties significantly, causing for instance in the W-Os region the change from oblate to prolate equilibrium shapes. In heavy nuclei, β_4 deformations play a significant role in determining the stability of heavy nuclei against fission and in predicting the existence and properties of super heavy nuclei. Recently, direct experimental information concerning β_2 and β_4 deformations in the actinide region has become available from inelastic scattering of protons and α particles above the Coulomb barrier^{8,9} and from Coulomb excitation experiments.¹⁰ Due to the significance of these findings and the high precision required in Coulomb excitation measurements, we felt it would be important to carry out an independent experiment on the easily available ^{232}Th isotope.

II. EXPERIMENTAL PROCEDURE AND CALCULATIONS

The experimental arrangement and procedure resemble those described in earlier papers of our group.^{11,12} α particles, accelerated to 16.5 and 17.0 MeV, were scattered from thin (10–20 $\mu\text{g}/\text{cm}^2$) 99.9% pure ^{232}Th spot targets on 20 $\mu\text{g}/\text{cm}^2$ carbon backings. A position sensitive Si detector placed at the focal plane of an Enge split-pole spectrograph was used to detect the back scattered projectiles at 143° lab angle. Additional data were

taken at 170.5° using a cooled, overbiased surface-barrier annular detector in a standard scattering chamber. A carefully designed beam-optics, and use of a pulse-pair rejector to prevent pileup effects guaranteed an energy resolution full width at half-maximum (FWHM) of 16–22 keV throughout the experiment. Two sample spectra are shown in Fig. 1.

For annular detector data peak shape analysis, that is separating elastic and inelastic peaks in order to determine $d\sigma_{2^+}/d\sigma_{0^+}$ and $d\sigma_{4^+}/d\sigma_{0^+}$ cross section ratios, was effected through a computer-coded self-consistent iterative method that assumed identical elastic and inelastic peak shapes.¹³ The method consists of varying relative height, as well as relative position of the 2^+ peak with respect to the elastic peak until the low energy tail of the elastic peak that falls under the 2^+ peak is a smoothly falling curve. The "identical-peak-shapes" assumption fails to hold true for the spectrograph data and a graphic hand analysis was used to replace the computer code in these instances. The $d\sigma_{2^+}/d\sigma_{0^+}$ values obtained from either type of data are believed to be accurate to within 1%. Uncertainties due to background subtraction as well as those associated with the lower statistics lead to somewhat larger uncertainties, i.e., 3–4%, in the $d\sigma_{4^+}/d\sigma_{0^+}$ ratios.

In evaluating the data, we assumed that the rigid-rotor model strictly holds for the low lying members of the ground state rotational band and various transition matrix elements can be, therefore, expressed in terms of the $\langle 0^+ || \mathfrak{M}(E2) || 2^+ \rangle$ and $\langle 0^+ || \mathfrak{M}(E4) || 4^+ \rangle$. To the extent that energy levels of the low lying members of the ground state rotational band follow the rigid-rotor model predictions only approximately, the second assumption holds exiguously. Deviations from the rigid-rotor

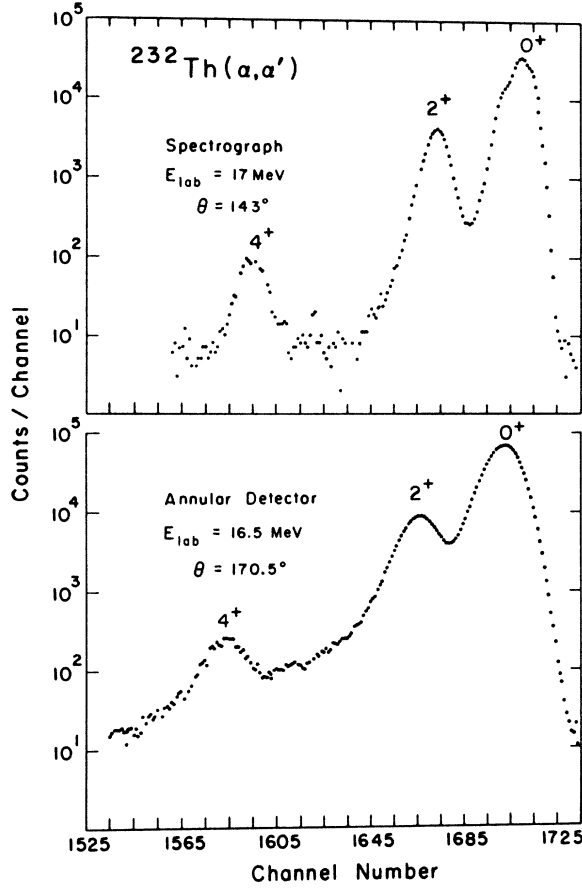


FIG. 1. Elastically and inelastically scattered α particles from ^{232}Th .

model, however, are not serious and the uncertainties in the $E4$ matrix elements due to possible deviations of $E2$ matrix elements from the rigid-rotor model predictions are well within the 12% quoted uncertainties.

Proceeding from these assumptions, the quantum mechanical coupled channel code AROSA¹⁴ was

TABLE I. Measured transition moments. The results labeled sc + qm_{corr} were obtained from a semiclassical evaluation to which quantum mechanical corrections were applied (see text).

	$\langle 0^+ \mathfrak{M}(E2) 2^+ \rangle$ (e b)	$\langle 0^+ \mathfrak{M}(E4) 4^+ \rangle$ (e b ²)
Pittsburgh		
Quant. mech.	3.035 ± 0.030	1.36 ± 0.14
sc + qm _{corr}	3.034 ± 0.030	1.24 ± 0.14
Oak Ridge ^a		
sc + qm _{corr}	3.035 ± 0.015	1.22 ± 0.15

^aC. E. Bemis *et al.*, Ref. 10.

used to extract the $E2$ and $E4$ reduced matrix elements. Included in these calculations were all possible $E2$ and $E4$ transitions among the 0^+ , 2^+ , and 4^+ levels. The effect of higher lying states, namely the 6^+ , 8^+ , and $2^{+'}$ states, is to modify the calculated reduced $E4$ matrix element by about 5%. To account for this effect the three-level quantum mechanical calculations were subsequently adjusted by application of correction factors. These correction factors were obtained by comparing the results of three-level and six-level calculations based on the semiclassical coupled channels code of Winther and deBoer.¹⁵

The sign for the reduced $E2$ matrix element was chosen to be positive to render a prolate quadrupole shape ($\beta_2 > 0$). The magnitude, as well as the sign for $\langle 0^+ || \mathfrak{M}(E4) || 4^+ \rangle$ are not, however, determined unambiguously. Given the $d\sigma_{4^+}/d\sigma_{0^+}$ cross section ratio, there are two solutions for the reduced $E4$ matrix element with opposite signs. In conformity with the theoretical calculations⁵⁻⁷ that predict a positive β_4 for ^{232}Th , we have adopted the positive solution. Reversal of this choice leads to considerably larger values for the $E4$ transition moments, which in turn give rise to physically unreasonable values for β_4 . A recent multiple Coulomb

TABLE II. Comparison of the extracted deformation parameters as obtained from this experiment with other work.

Work	β_2		β_4	
	Sharp surf.	Diffuse surf.	Sharp surf.	Diffuse surf.
Pittsburgh				
Quant. mech.	0.208 ± 0.006 ^a	0.229 ± 0.007 ^b	0.128 ± 0.018 ^a	0.137 ± 0.018 ^b
Semiclassical	0.211 ± 0.005 ^a	0.232 ± 0.006 ^b	0.115 ± 0.017 ^a	0.123 ± 0.018 ^b
Oak Ridge ^c	0.214 ± 0.005 ^d	0.238 ± 0.006 ^e	0.113 ± 0.018 ^d	0.130 ± 0.020 ^e
(p, p') ^f		0.23 ± 0.01		0.05 ± 0.015
Theory		0.206 ^g		0.084 ^g
		0.206 ^h		0.084 ^h

^a $R_0 = 1.2$ fm.

^b $R_0 = 1.1$ fm, $a = 0.6$ fm.

^cReference 10.

^d $R_0 = 1.2$ fm.

^e $R_0 = 1.10$ fm, $a = 0.50$ fm.

^fReference 8.

^gReference 6.

^hReference 7.

excitation experiment supports this choice, namely a positive value for the reduced $E4$ matrix element, independently.¹⁶ The extracted values for the reduced $E2$ and $E4$ matrix elements are shown in Table I. These values represent statistically weighted averages of various individual measurements.

To compare results of this experiment with the theoretical predictions and the reported measurements above the Coulomb barrier, we have extracted the model-dependent β_2 and β_4 (charge) deformation parameters. Required for this step is an assumption concerning the charge distribution $\rho(r, \theta)$. The connection between the $E2$ and $E4$ matrix elements and $\rho(r, \theta)$ is given by

$$\langle 0^+ \| \mathfrak{M}(E2) \| 2^+ \rangle = \int r^2 Y_{20}(\theta) \rho(r, \theta) d\tau,$$

$$\langle 0^+ \| \mathfrak{M}(E4) \| 4^+ \rangle = \int r^4 Y_{40}(\theta) \rho(r, \theta) d\tau.$$

Two different charge distributions, a (sharp surface) uniform charge distribution

$$\rho(r, \theta) = \begin{cases} \rho_0 & r \leq R(\theta) \\ 0 & r > R(\theta) \end{cases},$$

and a (diffuse surface) Fermi density

$$\rho(r, \theta) = \rho_0 / (1 + \exp\{[r - R(\theta)]/a\}),$$

where

$$R(\theta) = R_0 [1 + \beta_2 Y_{20}(\theta) + \beta_4 Y_{40}(\theta)]$$

were assumed to evaluate above integrals by exact numerical integration over a fine grid of β_2 and β_4 . In the above expression, the central charge density ρ_0 was held constant. The value for R_0 was varied to conserve the total charge as we changed the values of β_2 and β_4 over the grid. Appropriate interpolations were then applied to find values for β_2 and β_4 that reproduced the observed $E2$ and $E4$ matrix elements. The results, along with other reported values, are shown in Table II.

III. DISCUSSION

Table I summarizes the results for the transition moments. Included in the semiclassical calculations shown on the second line of the table are quantum mechanical corrections obtained from second order perturbation calculations.¹⁷ The $E4$ moment derived from the quantum mechanical calculations is $\sim 10\%$ larger than that obtained from quantum mechanically corrected semiclassical calculations. Also shown in Table I are the results of Bemis *et al.*¹⁰ which have been calculated using the latter procedure. The two sets of data are in excellent agreement.

In evaluating the data it was tacitly assumed that the excitation mechanism is purely Coulombian. In order to check this assumption we performed calculations using the coupled-channel Coulomb-nuclear interference code INTE.¹⁸ We have used the same optical potential parameters that were used by Brückner *et al.*¹⁹ in the rare earth region. The nuclear deformation parameters β_2^N and β_4^N were determined from the corresponding Coulomb deformation parameters using a relation recently given by Hendrie.²⁰ The results of these calculations are shown in Fig. 2 which shows that possible effects due to Coulomb-nuclear interference in the 16.5–17 MeV energy range are smaller than 0.5% and are therefore smaller than other uncertainties in the experiment. One observes on the other hand that the experiment cannot be carried out at a much higher energy without accounting for interference effects.

Table II indicates that the deformation parameter β_4^C obtained from Coulomb excitation is considerably larger than that obtained by Moss *et al.*⁸ from (p, p') scattering data above the Coulomb barrier, even after using the scaling procedure given by Hendrie.²⁰

Experiments, as well as calculations in the rare

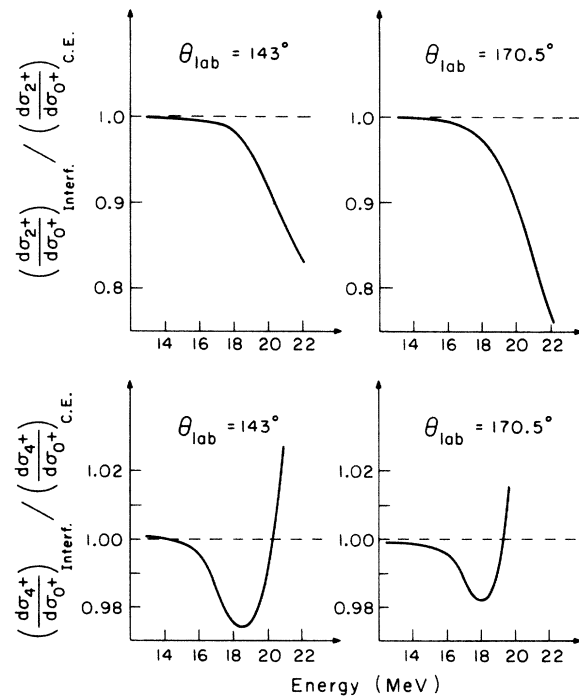


FIG. 2. Calculated Coulomb-nuclear interference effect in ^{232}Th . The optical potential parameters used in the calculation are $V = 47.0$ MeV, $W = 11.2$ MeV, $R = 8.666$ fm, $a = 0.605$ fm, $\beta_2^C = 0.232$, $\beta_2^N = 0.198$, $\beta_4^C = 0.123$, and $\beta_4^N = 0.095$.

earth region,²¹ have shown that Coulomb-nuclear interference phenomena are quite sensitive to differences between charge and nuclear deformation parameters. It would therefore be very desirable to extend the present measurements into this region.

ACKNOWLEDGMENT

It is a pleasure to acknowledge many helpful discussions we had with I. Y. Lee, J. O'Brien, and J. Holden. We also would like to thank them for their assistance in data taking.

†Work supported by the National Science Foundation.

¹P. O. Fröman, K. Dan. Vidensk. Selsk. Mat.-Fys. Skr. 1, No. 3 (1957).

²K. Kjallquist, Nucl. Phys. 9, 163 (1958).

³K. Harada, Phys. Lett. 10, 80 (1964).

⁴P. Möller, B. Nilsson, S. G. Nilsson, A. Sobiczewski, Z. Szymanski, and S. Wycech, Phys. Lett. 26B, 418 (1968).

⁵F. A. Gareev, S. P. Ivanova, and V. V. Pashkevitch, Yad. Fiz. 11, 1200 (1970) [transl.: Sov. J. Nucl. Phys. 11, 667 (1970)].

⁶S. G. Nilsson, C. F. Tsang, A. Sobiczewski, Z. Szymanski, S. Wycech, C. Gustafson, I. Lamm, P. Möller, and B. Nilsson, Nucl. Phys. A131, 1 (1969).

⁷H. Pauli, Phys. Rep. 7C, 35 (1973).

⁸J. M. Moss, Y. D. Terrien, R. M. Lombard, C. Brassard, J. M. Loiseaux, and F. Resmini, Phys. Rev. Lett. 26, 1488 (1971).

⁹D. L. Hendrie, B. G. Harvey, J. R. Meriwether, J. Mahoney, J. C. Faivre, and D. G. Kovar, Phys. Rev. Lett. 30, 571 (1973).

¹⁰C. E. Bemis, Jr., F. K. McGowan, J. L. C. Ford, Jr., W. T. Milner, P. H. Stelson, and R. L. Robinson, Phys. Rev. C 8, 1466 (1973).

¹¹T. K. Saylor, J. X. Saladin, I. Y. Lee, and K. Erb, Phys. Lett. 42B, 51 (1972).

¹²K. A. Erb, J. E. Holden, I. Y. Lee, J. X. Saladin, and T. K. Saylor, Phys. Rev. Lett. 29, 1010 (1972).

¹³T. K. Saylor, Ph.D. thesis, University of Pittsburgh, 1972 (unpublished).

¹⁴K. Alder, F. Roesel, and J. X. Saladin, J. Phys. Soc. Jap. Suppl. 34, 146 (1973); F. Roesel, J. X. Saladin, and K. Alder, Comput. Phys. Commun. (to be published).

¹⁵A. Winther and J. deBoer, in *Coulomb Excitation*, edited by K. Alder and A. Winther (Academic, New York, 1966).

¹⁶E. Eichler, N. R. Johnson, R. O. Sayer, D. C. Hensley, and L. L. Riedinger, Phys. Rev. Lett. 30, 568 (1973).

¹⁷K. Alder, F. Roesel, and R. Morf, Nucl. Phys. A186, 449 (1972).

¹⁸I. Y. Lee and J. X. Saladin, to be published.

¹⁹W. Brückner, J. G. Merdinger, D. Pelte, U. Smilansky, and K. Traxel, Phys. Rev. Lett. 30, 57 (1973).

²⁰D. L. Hendrie, Phys. Rev. Lett. 31, 478 (1973).

²¹I. Y. Lee, J. X. Saladin, J. E. Holden, C. Baktash, and J. O'Brien, Bull. Am. Phys. Soc. 18, 1388 (1973); and to be published.